NUCLEIC ACID THERAPEUTICS
Volume 25, Number 5, 2015

DOI: 10.1089/nat.2014.0528

Development and Application of an Ultrasensitive Hybridization-Based ELISA Method for the Determination of Peptide-Conjugated Phosphorodiamidate Morpholino Oligonucleotides

Umar Burki,[1] Jonathan Keane,[1] Alison Blain,[1] Liz O'Donovan,[2] Michael John Gait,[2] Steven H. Laval,[1] and Volker Straub[1]

Antisense oligonucleotide (AON)-induced exon skipping is one of the most promising strategies for treating Duchenne muscular dystrophy (DMD) and other rare monogenic conditions. Phosphorodiamidate morpholino oligonucleotides (PMOs) and 2′-*O*-methyl phosphorothioate (2′OMe) are two of the most advanced AONs in development. The next generation of peptide-conjugated PMO (P-PMO) is also showing great promise, but to advance these therapies it is essential to determine the pharmacokinetic and biodistribution (PK/BD) profile using a suitable method to detect AON levels in blood and tissue samples. An enzyme-linked immunosorbent assay (ELISA)-based method, which shows greater sensitivity than the liquid chromatography–mass spectrometry method, is the method of choice for 2′OMe detection in preclinical and clinical studies. However, no such assay has been developed for PMO/P-PMO detection, and we have, therefore, developed an ultrasensitive hybridization-based ELISA for this purpose. The assay has a linear detection range of 5–250 pM ($R^2 > 0.99$) in mouse serum and tissue lysates. The sensitivity was sufficient for determining the 24-h PK/BD profile of PMO and P-PMO injected at standard doses (12.5 mg/kg) in *mdx* mice, the dystrophin-deficient mouse model for DMD. The assay demonstrated an accuracy approaching 100% with precision values under 12%. This provides a powerful cost-effective assay for the purpose of accelerating the development of these emerging therapeutic agents.

Introduction

Antisense oligonucleotide (AON)-induced exon skipping is one of the most promising strategies for treating Duchenne muscular dystrophy (DMD) and other rare genetic diseases [1,2]. The first generation of AONs has now been tested in clinical trials for a number of genetic neuromuscular diseases and more trials are planned [3–6]. Several different chemistries of AONs are available [7] with 2′-*O*-methyl phosphorothioate (2′OMe) and phosphorodiamidate morpholino oligonucleotides (PMOs) being the AONs in the most advanced stages of development. Furthermore, the next generation of peptide-conjugated PMOs (P-PMOs) is also showing great promise in preclinical studies [8–11]. In addition to determining the efficacy, detection of the levels of AONs in biological samples such as blood and tissues is essential for determining the pharmacokinetic/pharmacodynamic (PK/PD) relationship. This, in turn, enables optimization of efficacy, while minimizing toxicity of the drug, thus significantly increasing the chances of successful development to a therapeutic drug.

Several detection methods have been developed over the years for quantifying AONs, such as high-performance liquid chromatography (HPLC) and, more recently, liquid chromatography–mass spectrometry (LC/MS) [12–17]. These methods have also been used for quantifying PMO in preclinical studies using HPLC [8] and clinical studies using LC/MS [5], with detection limits reported at 75 and 1 nM, respectively. In comparison, an enzyme-linked immunosorbent assay (ELISA)-based approach for detecting phosphorothioate (PTO) AONs has demonstrated far greater sensitivity with detection levels in the picomolar range [18,19]. The PTO ELISA was successfully adapted for detection of 2′OMe AONs, and as a result, this ELISA is currently the method of choice for 2′OMe detection in preclinical and clinical studies [6,20–22]. The 2′OMe ELISA is based on a

[1]The John Walton Muscular Dystrophy Research Centre, MRC Centre for Neuromuscular Diseases at Newcastle, Institute of Genetic Medicine, Newcastle University, Newcastle upon Tyne, United Kingdom.
[2]Laboratory of Molecular Biology, Medical Research Council, Cambridge, United Kingdom.

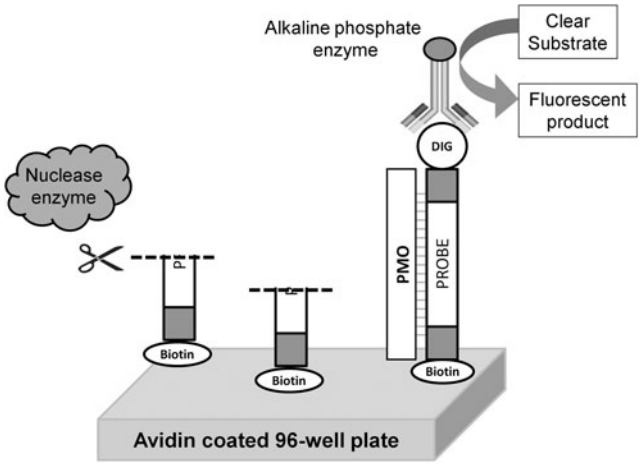

FIG. 1. Overview of the enzyme-linked immunosorbent assay (ELISA) principle based on hybridization of phosphorodiamidate morpholino oligonucleotides (PMO) with a dual-labeled DNA/phosphorothioate (PTO) probe.

hybridization principle first described by Yu *et al.*, where a complementary capture probe binds to the 2′OMe AON and then a detection probe is ligated to the AON [19]. In contrast, PMOs lack the OH-group at the terminal end, which is required for ligating the detection probe, and therefore, this approach cannot be used for PMOs. This may explain why a similar ELISA method has not been developed for PMO detection, and thus, LC/MS is currently the method of choice.

In this article, we report the first ELISA method for detecting PMO and P-PMOs in biological samples. The method has been adapted from a nuclease protection design first reported by Wei *et al.* in 2006 [18]. Briefly, the principle of the ELISA (shown in Fig. 1) is based on hybridization of PMO with a complementary DNA/PTO probe. The probe is dual labeled with a biotin and a digoxigenin at each end, where biotin is used to anchor the probe to NeutrAvidin-coated 96-well plates and digoxigenin is used for subsequent detection. The PMO/probe hybrids are differentiated from the single probe using micrococcal nuclease (MNase), which preferentially cleaves single-stranded DNA. The remaining hybrids are detected using the anti-digoxigenin antibody conjugated with an alkaline phosphatase enzyme, which converts a clear substrate into a fluorescent solution. The intensity of the fluorescence is determined using a fluorescence microplate reader, and a standard curve of PMO/P-PMO in the serum or tissue lysate is used to determine levels of each AON present in samples. The method presented here has been significantly modified from the original design, and as a result, the assay has a detection limit of 5 pM, which is 10-fold more sensitive than the original. The assay has been successfully validated in the mouse serum and tissue lysate and subsequently tested on *in vivo* samples to determine the pharmacokinetic and biodistribution (PK/BD) profile of both PMO and P-PMO in mice.

Materials and Methods

Animals

Mdx mice (C57BL/10-Dmd^{mdx}) were obtained from our own breeding facility and housed under controlled temperature (17°C–28°C) and light conditions (12-h light:12-h dark cycle). Animals had free access to food and water at all times. The investigations conformed with the Guide for the Care and Use of Laboratory Animals published by the US National Institutes of Health (NIH Publication No. 85–23, revised in 1985) and were performed under the terms of the Animals (Scientific Procedures) Act 1986, authorized by the Home Secretary, Home Office, UK. All experiments were performed at the Animal Care Facility of Newcastle University, and the work was approved by the Animal Welfare and Ethics Review Board of Newcastle University.

Materials and reagents

A 25-mer PMO antisense sequence for mouse dystrophin exon-23 (M23D) with sequence (5′GGCCAAACCTCGGC TTACCTGAAAT3′) and standard control PMO (5′CCTC TTACCTCAGTTACAATTTATA3′) was purchased from Gene Tools, Inc. (Philomath, OR). From here on the standard control PMO from Gene Tools will be referred to as the control PMO, and the M23D PMO will be used in all experiments where PMO was mentioned, unless otherwise stated. P-PMO was synthesized by conjugation of the M23D PMO with a cell-penetrating peptide Pip6a with the sequence RXRRB RRXRYQFLIRXRBRXRB (R, arginine; B, β-alanine; X, aminohexanoic acid), as previously described [23]. Pip6a-PMO was used in all P-PMO experiments. Complementary probes for both PMOs were sourced from Eurofins MWG Operon (Ebersberg, Germany). The probes for M23D PMO include a full-length DNA probe (3′CCGGTTTGGAGCC GAATGGACTTTA5′), a truncated DNA probe (3′CCGGTTT GGAGCCGAATGGAC5′), and a full-length PTO/DNA probe (3′**CCGGTTT**GGAGCCGAAT**GGACTTTA**5′), with phosphorothioate ends highlighted in bold. A complementary PTO/DNA probe was also designed for standard Gene Tools control PMO to be used in robustness and specificity studies (3′**GGAGAAT**GGAGTCAATGT**TAAATAT**5′). This will be referred to as the control probe. All probes were dual labeled with biotin at the 3′-end and digoxigenin at the 5′-end. The lyophilized probes were suspended in the Tris-EDTA (TE) buffer at 0.1 mM to prepare a stock solution, whereas PMO and P-PMO were suspended in distilled water at 1 and 0.1 mM stock, respectively. All probes and PMOs were kept at 4°C, whereas P-PMO was aliquoted and stored at −20°C. All probes, PMOs, and P-PMOs were heated at 65°C for 15 min and briefly vortexed before commencing the ELISA. Trypsin (Type II-s) was purchased from Sigma-Aldrich, Dorset (United Kingdom), as a lyophilized powder, resuspended in distilled water at 25 mg/mL, and supplemented with 100 mM CaCl to prevent autolysis. This generated a 10× stock that was stored at 20°C.

ELISA assay procedures

One hundred microliters of NeutrAvidin protein (Thermo Fisher, Leicestershire, United Kingdom) diluted in the carbonate–bicarbonate buffer (Sigma-Aldrich) at 1 μg/mL was used to coat 96-well black FLUOTRAC™ 600 plates (Greiner Bio-One, Gloucestershire, United Kingdom) at 100 ng/well. The plates were then sealed with polymerase chain reaction film and incubated at 37°C for 2 h, after which the plates were washed using a wash buffer (50 mM Tris-HCl, 150 mM sodium chloride, pH 7.6, 0.1% v/v Tween-20) and dried on absorbent paper. The same wash buffer is used for all

subsequent washing steps. PMO or P-PMO serial dilutions for a standard curve were made using the 1×TE buffer supplemented with 0.1% v/v Triton X-100 with a starting concentration of 2 nM PMO/P-PMO. A deep 0.8-mL 96-well plate was used for hybridizing PMO/P-PMO with a probe, where 100 µL of each dilution was added in duplicate wells followed by 100 µL of probe at 0.5 nM concentration in a hybridization buffer [1×TE buffer (Sigma-Aldrich) supplemented to 1 M final NaCl solution and 0.1% v/v Triton X-100]. The plate was then sealed and incubated at 37°C for 30 min to allow the probe to hybridize with the PMO/P-PMO. One hundred microliters of the hybridized solution was then transferred to the NeutrAvidin-coated plates and incubated at 37°C for 30 min to allow the biotin probe to bind to the NeutrAvidin-coated plate. The plate was then washed thrice and 150 µL of micrococcal nuclease [from New England BioLabs (Herts, United Kingdom) in 50 mM Tris-HCL (pH 8.2), 200 mM NaCl, 5 mM CaCl, and 0.1 mg/mL bovine serum albumin] was added at 30-U/well and incubated at 37°C for 1 h. This was sufficient to cleave at least 99% of the single-stranded probe consistently, as shown in Table 1. The plate was then washed thrice and 150 µL of anti-digoxigenin antibody conjugated with alkaline phosphatase (Roche, West Sussex, United Kingdom) was added at 1/5,000 dilution in the SuperBlock (TBS) Blocking Buffer (Thermo Fisher, Leicester, United Kingdom), together with 0.25% v/v Tween-20. The antibody was incubated at 37°C for 30 min followed by washing thrice. Then, the AttoPhos substrate (Promega, Hampshire, United Kingdom) was added at 150 µL/well, and the plates were sealed in aluminum foil and incubated at 37°C for 30 min. A Thermo Fluoroskan microplate reader by Thermo Fisher Scientific was used to determine the intensity of fluorescence at 444 nm excitation and 555 nm emission. Before reading, the plates were gently shaken in the reader at 2 mm radius/600 rpm for 10 s and the signal read at 500 ms delay per well.

Control serum and lysate preparation

Blood from 10 untreated *mdx* mice was extracted through cardiac bleed and collected in MiniCollect 0.8-mL serum tubes with a clot activator gel (Greiner Bio-One). This was allowed to clot for 30 min at 4°C before the samples were centrifuged at 16.2k rpm for 10 min to separate the serum from the blood. The serum was extracted, pooled, and aliquoted for storage at −20°C. For control tissue lysates, tissues were immediately removed and washed in phosphate-buffered saline before being dried on absorbent paper, weighed, and frozen whole at −20°C. For lysate preparation, the frozen tissues were thawed at room temperature, and then, the RIPA buffer (Thermo Fisher Scientific) supplemented with 2 mg/mL Proteinase-K (Roche) was added to each tissue at 100 mg/mL. The muscle lysate was made from a pool of various muscle tissues such as quadriceps (QD), tibialis anterior (TA), gastrocnemius (GST), and triceps (TCP). The tissues were homogenized using TissueRuptor® (Qiagen, West Sussex, United Kingdom) for a few seconds until the tissues were fully homogenized and the homogenate was then incubated at 55°C overnight. The homogenate was then centrifuged at 16.2k rpm for 15 min, and the supernatant was aliquoted and stored at −20°C ready for analysis.

Table 1. MNase Efficiency of Cleaving Single-Stranded Probe ($N=6$)

MNase (U/well)	*PMO mean ± SD*
120	99.6% ± 0.03%
30	99.4% ± 0.03%
8	99.1% ± 0.08%
2	98.2% ± 0.10%
0.5	96.2% ± 0.16%
0.12	89.1% ± 1.08%
0.03	56.4% ± 1.12%
0.01	22.6% ± 3.99%

MNase, micrococcal nuclease; PMO, phosphorodiamidate morpholino oligonucleotides; SD, standard deviation.

Determination of linear detection range

All dilutions of PMO/PPMO were performed in six replicate wells to determine the variability of the assay. Initially, the raw data are plotted with fluorescence intensity (FI) on the y-axis and PMO/PPMO concentration (pM) on the x-axis. However, the standard curve is better visualized after log transformation of the x-axis, which generates a typical sigmoidal curve. The y-axis is subsequently logged, which transforms the standard curve into a linear log–log graph and a power trendline is added. The linear detection range is determined by two factors, where the linear regression values must be above $R^2 > 0.99$ and the lower limit of quantitation (LLOQ) must be at least 2-fold above background control values. The latter is determined by a mean FI of wells, which only have probe and no PMO/P-PMO for protection, therefore the maximum probe is cleaved by nuclease. A two-tailed unpaired Student's *t*-test was also used to confirm statistical significance between LLOQ and control wells. This ensures a high degree of accuracy in determining concentrations of PMO/PPMO in samples.

Validation in serum and tissue lysate

The accuracy and precision of the assay were determined in the control serum and muscle lysate from untreated *mdx* mice diluted in the TE buffer at 5% concentration. The serum and muscle lysate was spiked with dilutions of P-PMO to 5, 10, 100, and 250 pM, which were selected to cover the entire linear detection range of the assay. The dilutions were analyzed in six replicates over 3 days for intraday ($n=6$) and interday ($n=18$) properties, respectively. The observed P-PMO values were determined from separate P-PMO calibration curves in both serum and muscle lysates. The accuracy of the assay was calculated using the observed values as a percentage of expected P-PMO concentration. The precision values (CV%) were determined using standard deviation within six replicates as a percentage of mean observed values.

Pharmacokinetic and biodistribution studies

The sensitivity of the assay to detect standard doses of both PMO and P-PMO was evaluated *in vivo* to determine the PK/BD profiles. *mdx* mice ($n=3$) were injected with 12.5 mg/kg P-PMO or 9.4 mg/kg of equimolar PMO through the subcutaneous route at 5 mL/kg volume under anesthesia. PMO and P-PMO were each mixed with saline immediately before the

Table 2. Dilutions of Serum Samples Required for PK Analysis

Time (min)	*PMO and P-PMO (final dilutions in TE buffer)*		
5	1/1,000	1/4,000	1/16,000
15	1/3,000	1/12,000	1/48,000
30	1/3,000	1/12,000	1/48,000
60	1/3,000	1/12,000	1/48,000
180	1/300	1/1,200	1/4,800
420	1/100		
1440	1/10	1/20	1/40

PK, pharmacokinetic; P-PMO, peptide-conjugated PMO; TE, Tris-EDTA.

injections. Serum sampling for PK analysis was carried out using heparinized capillary tubes calibrated at 15 μL volume from BHR Pharmaceuticals (Nuneaton, United Kingdom). Fifteen microliters of blood samples from the saphenous vein in the hind limbs of each mouse was collected at 5, 15, 30, 60, 180, and 420 min after injection. The blood was allowed to clot for 30 min at 4°C before the samples were centrifuged at 16.2k rpm for 10 min to separate the serum from blood. Five microliters of serum was consistently extracted from each sample and diluted 1/100 in the TE buffer. In contrast, the 24-h blood sample was collected through cardiac bleed before the animal was sacrificed through cervical dislocation, and the serum was stored undiluted with rest of the serum samples at −20°C. For PK analysis, a standard curve for each PMO/P-PMO was prepared using 1% and 10% control serum diluted in the TE buffer. One percentage of serum was used to dilute all the serum samples collected at 5, 15, 30, 60, and 180 min to ensure that the background serum concentration remains the same. Whereas 10% control serum was used to dilute the 24-h serum sample. To determine the appropriate dilutions required for each sample, an initial range-finding study was performed. Based on that information (data not shown), the following dilutions were selected (Table 2) that would allow three dilutions at each time point to be detected. The dilutions stated in Table 2 are final dilutions of serum samples, and each sample was analyzed in duplicate.

Immediately after sacrificing, the animal tissues were harvested for BD analysis, including the kidney, liver, heart, diaphragm, QD, GST, TA, TCP, and brain. Tissues were subsequently stored and lysed as described earlier for preparing the control lysate. For BD analysis, a standard curve for each PMO/P-PMO was prepared using control liver, kidney, heart, brain, and pooled muscle lysates. Tissue lysate samples from treated *mdx* mice were diluted 1/20 in 5% control heart, brain, and pooled muscle lysates. By contrast, liver lysate samples were diluted at 1/200, and kidney samples were diluted at 1/5,000 in 1% control lysate. Each sample was subsequently diluted 2-fold to get three dilutions of each sample, and each sample was analyzed in duplicate.

Results

Optimization of probe design

Initially, a full-length 25-mer complementary DNA probe was used to develop the ELISA. However, this resulted in probe/PMO hybrids, which were not sufficiently resistant to nuclease digestion, leading to a poor detection range from 16 to 500 pM PMO (Fig. 2E). This was subsequently found to be

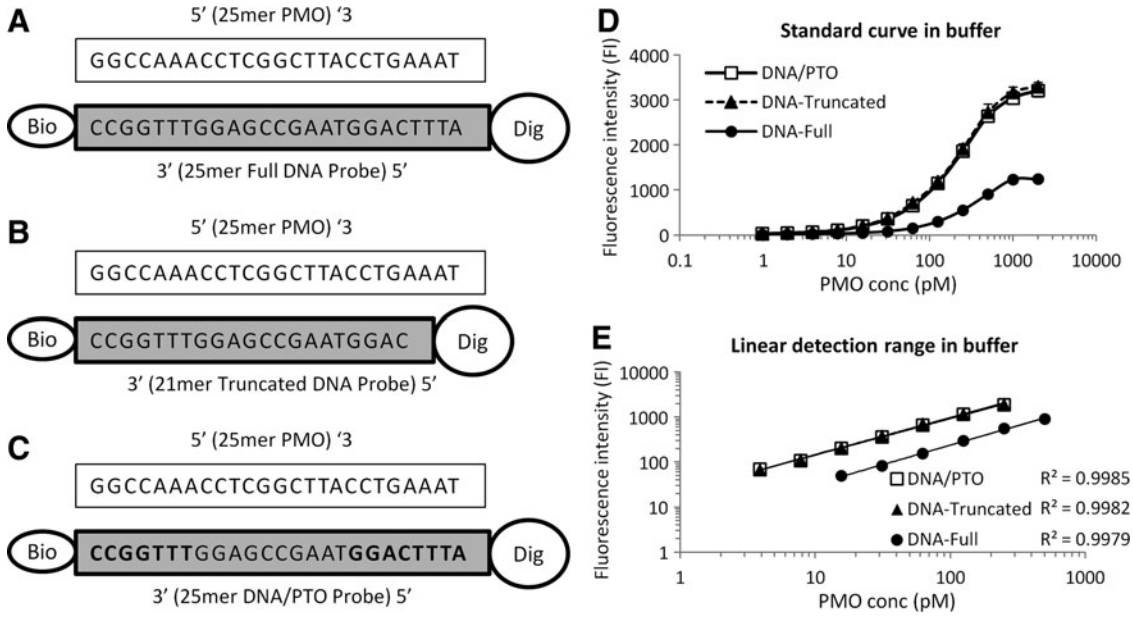

FIG. 2. The complementary probe designed to capture and detect PMO was optimized from a full-length 25-mer DNA probe **(A)** to a slightly truncated 21-mer probe **(B)**. The ends of the full-length probe were also replaced with nuclease-resistant PTO terminal ends, highlighted in bold **(C)**. The stability of all three probes is illustrated with a standard curve in Tris-EDTA (TE) buffer **(D)** and the linear detection range with regression values **(E)**. The lower limit of quantitation (LLOQ) for all three probes was more than 2-fold above their respective control values (ie, without PMO), which was statistically significant (*t*-test $P < 0.001$). Each PMO dilution was analyzed in six replicate wells, and horizontal bars represent standard deviation (SD) error values.

due to a 4-mer region composed of AT bases located at the 5′-end of the probe, which is the preferred cleavage site for most nuclease enzymes. In addition, the location of this region at the end of the probe makes it particularly vulnerable to nuclease attack, since double-stranded nucleic acid molecules are generally prone to melting at the ends. Therefore, the four AT bases were omitted from the second probe design, which was slightly truncated relative to the original, but produced considerably more nuclease-resistant hybrids, resulting in a wider and more sensitive detection range from 4 to 500 pM PMO (Fig. 2D). This confirmed that the AT region was being cleaved too readily by the nuclease for the probe/PMO hybrid to be detected. However, the probe was further improved by replacing the terminal ends of the full probe with a phosphorothioate backbone, which is resistant to nuclease attack. This resulted in a similar detection range to that of the

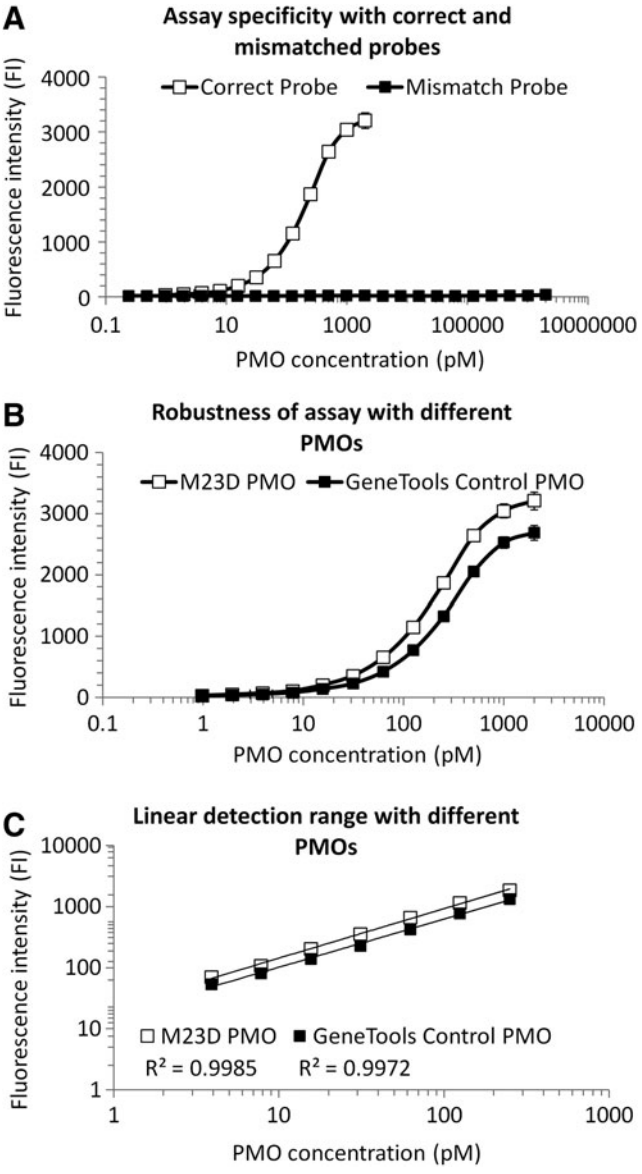

FIG. 3. Specificity and robustness of assay in TE buffer. **(A)** High degree of specificity is shown when the mouse dystrophin exon-23 (M23D) probe is hybridized correctly with its complementary M23D PMO up to 2 nM. In contrast, mismatched control PMO was not significantly detected even up to 2,000 nM concentrations. **(B, C)** Robustness of the assay is shown as a standard curve of M23D PMO and control PMO with their respective complementary probes as a semilog graph **(B)** and the resulting log–log graph to determine the linear detection range **(C)**. Both PMOs showed a similar detection range, which was between 4 and 500 pM. The LLOQ (4 pM) for both PMOs was over 2-fold above their respective control values (*t*-test $P < 0.001$). Each PMO dilution was analyzed in six replicate wells, and horizontal bars represent SD error values.

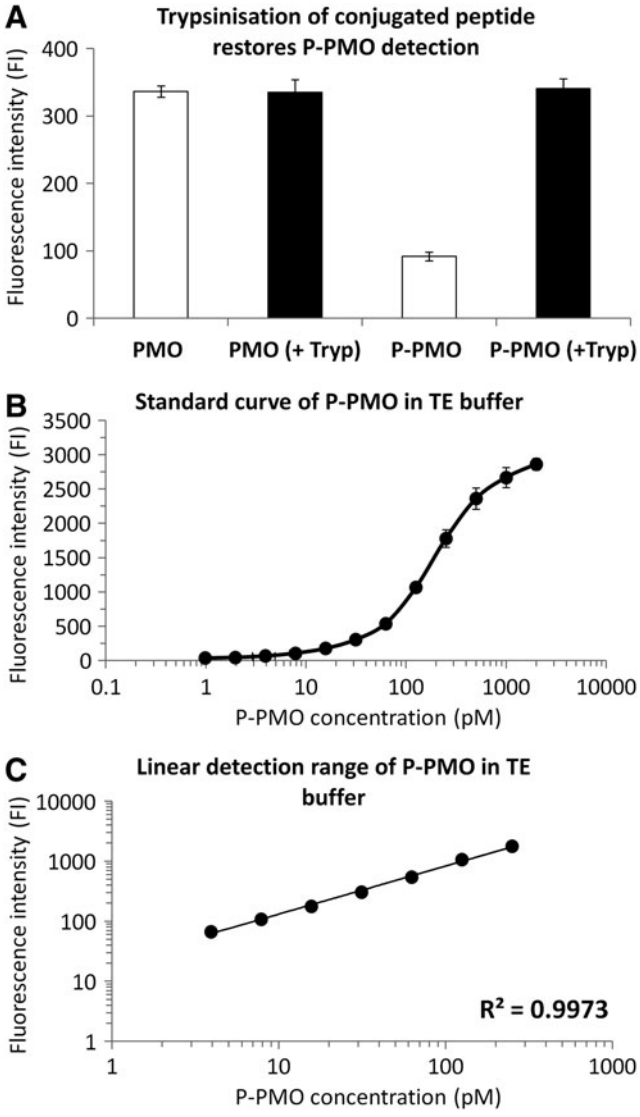

FIG. 4. Optimization of peptide-conjugated PMO (P-PMO) detection in TE buffer. **(A)** Trypsinization of conjugated peptide restores detection of 250 pM P-PMO in TE buffer. **(B, C)** A typical standard curve of P-PMO is shown as a semilog graph and the resulting log–log graph to determine the linear detection range, which was between 4 and 250 pM. The LLOQ (4 pM) over was 2-fold above the respective control values (*t*-test $P < 0.001$). Each PMO dilution was analyzed in six replicate wells, and horizontal bars represent SD error values.

truncated probe (Fig. 2E), and therefore, it was selected for development of the assay throughout the remainder of the study.

Specificity and robustness of assay

The assay was validated for specificity and robustness using a control PMO and its complementary control probe. For the specificity test, a 0.5 nM M23D probe was hybridized with M23D PMO or control PMO diluted by 2-fold serial dilutions in the TE buffer starting from 2 or 2,000 nM concentrations, respectively. The data show a high degree of specificity up to 1,000-fold higher concentrations of the mismatched control PMO (Fig. 3A). Even at the highest concentration of the control PMO, the FI was still within 2-fold above background values (ie, without PMO) and, therefore, not considered significant. The robustness of the assay was tested using control PMO, and M23D PMO was hybridized with their correct complementary probes (Fig. 3B). A similar standard curve and detection range (4–500 pM) were observed for both PMOs, suggesting that the assay is robust.

Optimizing the assay in buffer

To determine the best detection range and sensitivity for PMO, the ELISA was first optimized in a buffer without tissue or serum present. For P-PMO detection, an additional step was required, since the peptide portion of the P-PMO was found to interfere with the assay. This was easily overcome using overnight incubation with 2.5 mg/mL trypsin at 37°C before running the ELISA (Fig. 4A). The data show high sensitivity and a wide detection range of 5–250 pM for P-PMO detection in the TE buffer (Fig. 4B, C).

Validation in serum and tissue lysate

The assay was validated to determine detection range, accuracy, and precision in serum and tissue lysates. A similar detection range as found in the TE buffer was observed for P-PMO in 5% serum, which shows a typical semilog standard curve and log–log linear detection range from 4 to 125 pM (Fig. 5). Both PMO and P-PMO detection ranges were tested in various control tissue lysates. Tissue lysates were used at a 1/20 dilution of lysate in the TE buffer, giving a final tissue concentration of 5 mg/mL. However, both kidney and liver lysates were further diluted to 1/100 (ie, 1 mg/mL), since higher concentrations were found to interfere with the avidin coating and, thus, significantly reduce the binding of biotinylated probe (data not shown). The ELISA showed a high degree of sensitivity and linearity in all tissues tested, with detection limits as low as 1 pM (Table 3). However, this level of sensitivity was not always reproducible, and therefore, to determine the accuracy and precision of the assay, 5 pM was selected as the LLOQ. There is little variation in detection ranges of PMO and P-PMOs in various tissues lysates (Table 3). Therefore, accuracy and precision tests carried out using P-PMO diluted in serum and muscle lysate are expected to be comparable to PMO/P-PMO diluted in other tissue lysates. The results show a high degree of accuracy (approaching 100%) and precision (under 12% variability) in the 5–250 pM detection range for P-PMO in the serum and muscle lysate at a 1/20 dilution (Table 4).

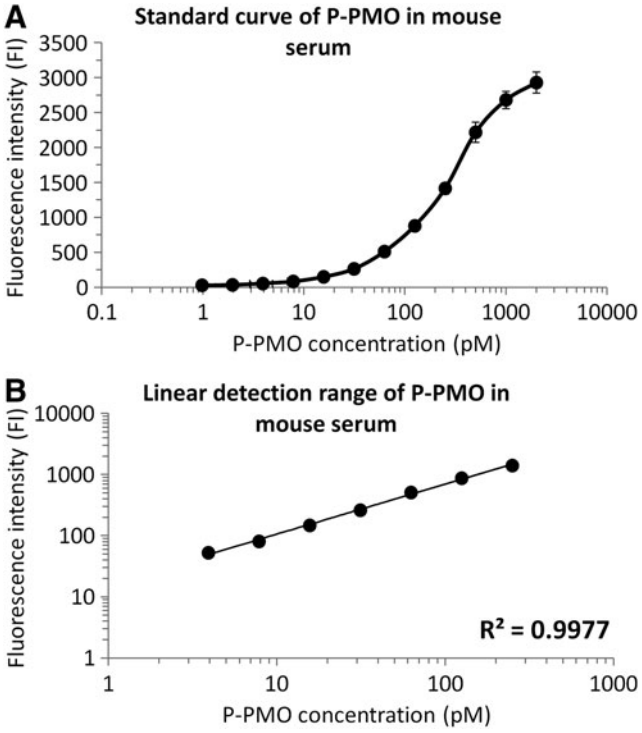

FIG. 5. Validation of P-PMO detection by ELISA in control *mdx* mouse serum. A typical standard curve of P-PMO in 10% *mdx* mouse serum is shown as a semilog graph **(A)** together with the linear detection range in a log–log graph, with a detection range of 4–250 pM **(B)**. The LLOQ (4 pM) over was 2-fold above the respective control values (*t*-test $P < 0.001$). Each PMO dilution was analyzed in six replicate wells and horizontal bars represent SD error values.

Pharmacokinetic and biodistribution analysis

Analysis of serum samples from treated *mdx* mice shows that the assay is sufficiently sensitive to monitor levels of both PMO and P-PMO throughout the 24-h period (Fig. 6A). Even at the lowest levels, both P-PMO (2296.9 ± 164.4 pM) and PMO (143.8 ± 7.1 pM) were well above the lower detection limit of 5 pM. This shows that the sensitivity of the assay is more than adequate for 24-h PK profiling in individual *mdx* mice at standard doses of PMO and P-PMO. Various PK parameters were calculated from the data and

Table 3. Summary of Linear Detection Range in Various Mouse Tissue Lysates Spiked with PMO and P-PMO

	Linear detection range (pM)			
Tissue lysate	*PMO (min–max)*	R^2	*P-PMO (min–max)*	R^2
Kidney	1–125	> 0.9977	2–250	> 0.9985
Liver	1–125	> 0.9986	2–250	> 0.9978
Heart	1–125	> 0.9983	1–250	> 0.9964
Muscle	1–125	> 0.9989	2–250	> 0.9980
Diaphragm	2–125	> 0.9983	2–500	> 0.9970
Brain	1–125	> 0.9981	1–250	> 0.9976

Table 4. Accuracy and Precision of P-PMO in Mouse Serum and Muscle Lysate

		Serum			*Muscle*		
ID	*Nominal conc. (pM)*	*Observed conc. (pM) (mean ± SD)*	*Accuracy (%)*	*Precision (CV%)*	*Observed conc. (pM) (mean ± SD)*	*Accuracy (%)*	*Precision (CV%)*
Intraday ($n=6$)							
Max QC	250	211.5 ± 18.0	84.6	8.5	248.0 ± 21.1	99.2	8.5
Mid QC	100	81.2 ± 10.6	81.2	13.0	114.2 ± 12.8	114.2	11.2
Low QC	10	8.7 ± 0.3	87.4	3.5	10.6 ± 0.8	105.5	7.7
LLQC	5	5.1 ± 0.2	101.1	3.2	4.5 ± 0.6	90.7	12.4
Interday ($n=18$)							
Max QC	250	266.8 ± 32.8	106.7.	12.3	216.5 ± 24.2	86.6	11.2
Mid QC	100	105.5 ± 20.9	105.5	19.8	92.4 ± 16.4	92.4	17.8
Low QC	10	11.3 ± 0.9	112.8	7.7	10.5 ± 1.7	104.8	16.1
LLQC	5	5.5 ± 0.7	110.1	12.4	5.3 ± 1.1	105.3	21.3

LLOQ, lowest limit of quantification; QC, quality control; CV, coefficient of variation.

presented in Table 5. Overall, there were many similarities, but the major difference was the slower absorbance and clearance of P-PMO compared to PMO. This resulted in an ~3-fold greater drug exposure of P-PMO than PMO. BD profile was determined by analyzing PMO and P-PMO levels in the lysate from a broad spectrum of tissues (Fig. 6B). As expected, the vast majority of both P-PMO and PMO were taken up by the kidney and liver, which are consistent with previous findings [8]. P-PMO levels were generally 3- to 10-fold higher than PMO in all tissues studied. However, there was a particularly high uptake in the liver, where P-PMO was over 130-fold higher than PMO. Surprisingly, in contrast to PMO, P-PMO was also detected in the brain, although at low levels.

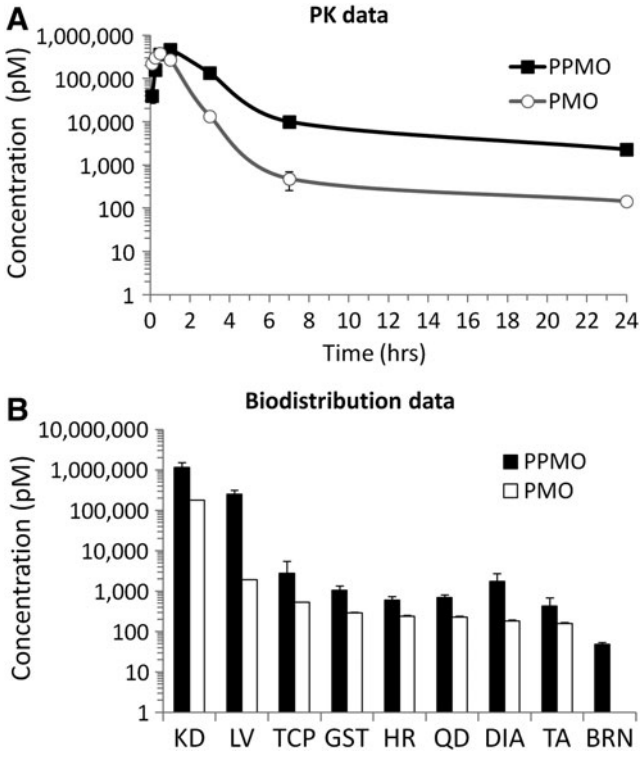

FIG. 6. *In vivo* validation of the assay showing the pharmacokinetic **(A)** and biodistribution **(B)** data in *mdx* mice ($n=3$) injected with equimolar doses of PMO (9.4 mg/kg) and P-PMO (12.5 mg/kg). KD, kidney; LV, liver; TCP, triceps; GST, gastrocnemius; HR, heart; QD, quadriceps; DIA, diaphragm; TA, tibialis anterior; BRN, brain. Horizontal bars represent SD values between three means.

Discussion

Preclinical and clinical research strategies aiming to develop AON treatments for patients with genetic diseases are in need of a highly sensitive detection method to determine PK/BD profiles for PMO and P-PMO. We developed an ultrasensitive hybridization-based ELISA assay and applied it in the mouse model for DMD.

The most challenging aspect during development of this assay was stabilizing the PMO/probe hybrids in a manner resistant to nuclease cleavage. This was mainly due to the conditions required for maintaining stable hybrids, which affected the activity of the nucleases tested. Nucleic acid hybrids are most stable in the presence of high salt (>100 mM) and at neutral pH. The nuclease originally used by Wei *et al.* was the S1 nuclease, which is highly sensitive to pH and significantly loses activity at pH > 4.5 [18]. Therefore, this was replaced by MNase, which is less sensitive to pH changes and has a working range of pH 7–10. However, even MNase is not ideal because it only has a preference for single-stranded DNA and will cleave double-stranded DNA, especially at higher concentrations [25,26]. Therefore, it was also necessary to stabilize the terminal ends of the hybrids, which

Table 5. PK Analysis of PMO and P-PMO Levels in Serum Following Subcutaneous Administration in *mdx* mice

Parameter	*PMO mean ± SD*	*P-PMO mean ± SD*
C_{max} (nM)	379.5 ± 55.6	443.0 ± 32.3
t_{max} (min)	30.0 ± 10.0	54.0 ± 12.0
$t_{1/2}$ (min)	61.7 ± 8.6	74.0 ± 9.2
AUC (h × mg/L)	4190.3 ± 531.8	12922.5 ± 862.7

C_{max}, maximum concentration; t_{max}, time to reach maximum concentration; $t_{1/2}$, half-life; AUC, area under curve as calculated using linear trapezoidal rule.

generally have a tendency to melt. This was most effectively achieved by replacing the terminal ends of the DNA probe with a PTO backbone to make the PMO/probe hybrids resistant to cleavage, except in the central portion. This was found to be just as effective as the truncated DNA probe, but offers additional advantages. The phosphorothioate ends ensure that the nuclease attack is targeted in the center of the probe, thereby strengthening the terminal ends of the probe/PMO hybrid. This also enables the full-length probe to be used rather than a truncated probe, resulting in stronger hybrids. Finally, it allows detection of other PMO sequences that may be developed for other targets, which may have longer AT regions at terminal ends, without the need for further truncating the DNA probe. Overall, the modifications made to the probe and nuclease have helped to develop a more robust hybrid.

The optimized M23D probe was used to determine the sequence specificity of the assay using a control PMO with a 40% sequence homology with M23D PMO. Even at concentrations 1,000-fold greater than M23D PMO, the nonspecific interference of control PMO was within 2-fold of background levels and, therefore, not considered significant. Furthermore, the control PMO was subsequently hybridized with the correct complementary control probe and this resulted in a similar detection range as observed with M23D PMO (ie, 4–500 pM). Together, both findings demonstrate the high specificity and robustness of the assay in detecting the PMO of interest.

The assay also demonstrated a high degree of sensitivity, accuracy, and precision with a detection range of 5–250 pM, which is 10-fold more sensitive compared to similar ELISA methods [18,19]. To the best of our knowledge, no other ELISA-based approach has been developed for detection of PMO, except for a recent flow cytometry-based method. Schnell *et al.* published a similar hybridization assay to the ligation ELISA design, which is detected using flow cytometry [27]. The assay reported a wide detection range of PMO between 0.4 and 400 nM, which means that the present assay is still 80-fold more sensitive in comparison.

In comparison to PTO-containing AONs, PMOs are widely considered to be more resistant to degradation both *in vitro* and *in vivo* [28–30]. Therefore, it was not considered necessary to test interference from possible metabolic products of PMO. The PMO detected by this assay is expected to be mostly intact and, thus, in its active form. The assay was successfully validated in 10% mouse serum and 5 mg/mL tissue lysate dilution, which showed a similar detection range as found in the TE buffer. However, due to the high sensitivity of the assay, higher concentrations of serum and tissue lysate were found to significantly increase the background and to decrease the sensitivity. Nonetheless, these dilutions were found to be sufficient for determining PK-BD of PMO and P-PMO in *mdx* mice at standard doses. This demonstrates that serum and tissue lysate tolerance is adequate for most *in vivo* applications, where PMO and P-PMO are measured 24 h after last administration.

Analysis of the PK data shows that P-PMO is cleared more slowly and has a 3-fold greater drug exposure than PMO, which is consistent with previous comparisons [8]. Overall, P-PMO has a more favorable PK profile than PMO for optimum tissue uptake. Both AONs were easily detected in various tissue lysates to enable a comprehensive BD profile to be determined. Consistent with previous findings [8], the data show that peptide conjugation facilitated the delivery of the PMO to all tissues, including a marked increase in liver uptake, where P-PMO was detected 130-fold higher than PMO. This will no doubt be of great concern with regard to possible adverse effects of subsequent dosing and drug accumulation in the liver. This highlights the utility of such an assay where tissue retention studies can help optimize the dosing regimen for maximum efficacy and minimal toxicity.

One of the major limitations of PMO and P-PMO is the poor efficacy generally observed in the heart and diaphragm compared to muscle tissue [8,10,11,31]. Interestingly, the BD data presented here show comparable levels of PMO and P-PMO in these tissues, which seem to suggest that the poor efficacy may not be due to poor delivery of these AONs to the heart and diaphragm, but rather tissue-specific factors affecting efficacy, such as cellular and subcellular uptake [32,33]. The concentration of PMO and P-PMO in subcellular compartments is expected to be much lower than in the whole tissue lysate and, therefore, would require even greater sensitivity of detection than needed for the whole tissue lysate. Currently, this ELISA is the most sensitive detection method available and it can be used with existing subcellular fractionation methods to determine the subcellular location of PMO and P-PMO in various tissues. This would help in the process of optimizing the design of PMO and P-PMO for enhanced intracellular delivery and efficacy.

Surprisingly, P-PMO, but not PMO, was also detected in the brain, which was not considered possible due to such molecules being thought to be unable to cross the blood–brain barrier (BBB) because of their large size. However, there is some mixed evidence in the literature that seems to suggest that P-PMOs may be able to cross the BBB. Studies utilizing transgenic mice expressing an aberrantly spliced enhanced green fluorescence protein serving as a reporter for the presence of a P-PMO designed to correct the splicing error report similar BD profiles as seen in the present study; however, they did not detect any P-PMO in the brain [9,34]. By contrast, a more recent study employed fluorescein isothiocyanate (FITC)-labeled P-PMO to determine tissue uptake in mice that showed P-PMO uptake in the brain [35]. However, this needs to be cautiously interpreted since the FITC was labeled at the peptide portion of the P-PMO, which is vulnerable to the metabolism *in vivo* [8]. Therefore, it is possible that the peptide was cleaved from the PMO, and thus, only the FITC-labeled peptide fragment was able to cross the BBB. By contrast, the present assay is a direct assessment of P-PMO in the brain and it is unaffected by the peptide metabolism *in vivo*. The present findings in the brain are also interesting since there is ever growing focus on the role of dystrophin in the brain [36,37], and therefore, it will be of great therapeutic significance if P-PMOs are able to cross the BBB. Therefore, to confirm these findings, further studies are needed where P-PMO is given chronically and brain uptake is compared in *mdx* mice. If there is accumulation of P-PMO in the brain, then it would strongly suggest that P-PMOs are able to penetrate the BBB. Comparison with wild-type mice will also confirm whether there are differences in uptake between healthy and dystrophic mice due to a compromised BBB [38].

During a recent PMO clinical trial in DMD boys, LC/MS was used to detect PMO in plasma for determining the PK

profile of various doses [5]. Only the highest 20 mg/kg dose was detected after 24 h, and lower doses were detected just over 8–12 h. In comparison, the present assay has a 200-fold lower threshold for detection and, therefore, should be sufficiently sensitive to detect PMO over 24 h, even at low doses. Overall, this suggests that the assay will be a radical improvement over existing technologies for both preclinical and clinical applications, which will greatly facilitate the development of these AONs.

Acknowledgments

We acknowledge the support of the Sylvia Aitken Charitable Trust in funding this work. M.J.G. and V.S. are members of the MDEX consortium. Work in the laboratory of M.J.G. was supported by the Medical Research Council (MRC program number U105178803).

Author Disclosure Statement

The authors have no relevant affiliations or financial involvement with any organization or entity with a financial interest in or financial conflict with the subject matter or materials discussed in the article. This includes employment, stock ownership or options, expert testimony, patents received or pending, or royalties. However, M.J.G. declares interest in a patent application on the design and use of Pip6a-PMO.

References

1. Siva K, G Covello and MA Denti. (2014). Exon-skipping antisense oligonucleotides to correct missplicing in neurogenetic diseases. Nucleic Acid Ther 24:69–86.
2. Veltrop M and A Aartsma-Rus. (2014). Antisense-mediated exon skipping: taking advantage of a trick from Mother Nature to treat rare genetic diseases. Exp Cell Res 325: 50–55.
3. van Deutekom JC, AA Janson, IB Ginjaar, WS Frankhuizen, A Aartsma-Rus, M Bremmer-Bout, JT den Dunnen, K Koop, AJ van der Kooi, *et al.* (2007). Local dystrophin restoration with antisense oligonucleotide PRO051. N Engl J Med 357:2677–2686.
4. Kinali M, V Arechavala-Gomeza, L Feng, S Cirak, D Hunt, C Adkin, M Guglieri, E Ashton, S Abbs, *et al.* (2009). Local restoration of dystrophin expression with the morpholino oligomer AVI-4658 in Duchenne muscular dystrophy: a single-blind, placebo-controlled, dose-escalation, proof-of-concept study. Lancet Neurol 8:918–928.
5. Cirak S, V Arechavala-Gomeza, M Guglieri, L Feng, S Torelli, K Anthony, S Abbs, ME Garralda, J Bourke, *et al.* (2011). Exon skipping and dystrophin restoration in patients with Duchenne muscular dystrophy after systemic phosphorodiamidate morpholino oligomer treatment: an open-label, phase 2, dose-escalation study. Lancet 378: 595–605.
6. Goemans NM, M Tulinius, JT van den Akker, BE Burm, PF Ekhart, N Heuvelmans, T Holling, AA Janson, GJ Platenburg, *et al.* (2011). Systemic administration of PRO051 in Duchenne's muscular dystrophy. N Engl J Med 364:1513–1522.
7. Saleh AF, AA Arzumanov and MJ Gait. (2012). Overview of alternative oligonucleotide chemistries for exon skipping. Methods Mol Biol 867:365–378.
8. Amantana A, HM Moulton, ML Cate, MT Reddy, T Whitehead, JN Hassinger, DS Youngblood and PL Iversen. (2007). Pharmacokinetics, biodistribution, stability and toxicity of a cell-penetrating peptide-morpholino oligomer conjugate. Bioconjug Chem 18:1325–1331.
9. Jearawiriyapaisarn N, HM Moulton, B Buckley, J Roberts, P Sazani, S Fucharoen, PL Iversen and R Kole. (2008). Sustained dystrophin expression induced by peptide-conjugated morpholino oligomers in the muscles of mdx mice. Mol Ther 16:1624–1629.
10. Yin H, HM Moulton, C Betts, Y Seow, J Boutilier, PL Iverson and MJ Wood. (2009). A fusion peptide directs enhanced systemic dystrophin exon skipping and functional restoration in dystrophin-deficient mdx mice. Hum Mol Genet 18:4405–4414.
11. Yin H, HM Moulton, C Betts, T Merritt, Y Seow, S Ashraf, Q Wang, J Boutilier and MJ Wood. (2010). Functional rescue of dystrophin-deficient mdx mice by a chimeric peptide-PMO. Mol Ther 18:1822–1829.
12. Bigelow JC, LR Chrin, LA Mathews and JJ McCormack. (1990). High-performance liquid chromatographic analysis of phosphorothioate analogues of oligodeoxynucleotides in biological fluids. J Chromatogr 533:133–140.
13. Leeds JM, MJ Graham, L Truong and LL Cummins. (1996). Quantitation of phosphorothioate oligonucleotides in human plasma. Anal Biochem 235:36–43.
14. Reyderman L and S Stavchansky. (1996). Determination of single-stranded oligodeoxynucleotides by capillary gel electrophoresis with laser induced fluorescence and on column derivatization. J Chromatogr A 755:271–280.
15. Chen S-H, M Qian, JM Brennan and JM Gallo. (1997). Determination of antisense phosphorothioate oligonucleotides and catabolites in biological fluids and tissue extracts using anion-exchange high-performance liquid chromatography and capillary gel electrophoresis. J Chromatogr B Biomed Sci Appl 692:43–51.
16. Gaus HJ, SR Owens, M Winniman, S Cooper and LL Cummins. (1997). On-line HPLC electrospray mass spectrometry of phosphorothioate oligonucleotide metabolites. Anal Chem 69:313–319.
17. Griffey RH, MJ Greig, HJ Gaus, K Liu, D Monteith, M Winniman and LL Cummins. (1997). Characterization of oligonucleotide metabolism in vivo via liquid chromatography/electrospray tandem mass spectrometry with a quadrupole ion trap mass spectrometer. J Mass Spectrom 32:305–313.
18. Wei X, G Dai, G Marcucci, Z Liu, D Hoyt, W Blum and KK Chan. (2006). A specific picomolar hybridization-based ELISA assay for the determination of phosphorothioate oligonucleotides in plasma and cellular matrices. Pharm Res 23:1251–1264.
19. Yu RZ, B Baker, A Chappell, RS Geary, E Cheung and AA Levin. (2002). Development of an ultrasensitive noncompetitive hybridization-ligation enzyme-linked immunosorbent assay for the determination of phosphorothioate oligodeoxynucleotide in plasma. Anal Biochem 304:19–25.
20. Verhaart IE, L van Vliet-van den Dool, JA Sipkens, SJ de Kimpe, IG Kolfschoten, JC van Deutekom, L Liefaard, JE Ridings, SR Hood and A Aartsma-Rus. (2014). The dynamics of compound, transcript, and protein effects after treatment with 2OMePS antisense oligonucleotides in mdx mice. Mol Ther Nucleic Acids 3:e148.
21. Heemskerk HA, CL de Winter, SJ de Kimpe, P van Kuik-Romeijn, N Heuvelmans, GJ Platenburg, GJ van Ommen,

JC van Deutekom and A Aartsma-Rus. (2009). In vivo comparison of 2′-O-methyl phosphorothioate and morpholino antisense oligonucleotides for Duchenne muscular dystrophy exon skipping. J Gene Med 11:257–266.
22. Verhaart IE, CL Tanganyika-de Winter, TG Karnaoukh, IG Kolfschoten, SJ de Kimpe, JC van Deutekom and A Aartsma-Rus. (2013). Dose-dependent pharmacokinetic profiles of 2′-O-methyl phosphorothioate antisense oligonucleotidesin mdx mice. Nucleic Acid Ther 23:228–237.
23. Betts C, AF Saleh, AA Arzumanov, SM Hammond, C Godfrey, T Coursindel, MJ Gait and MJ Wood. (2012). Pip6-PMO, a new generation of peptide-oligonucleotide conjugates with improved cardiac exon skipping activity for DMD treatment. Mol Ther Nucleic Acids 1:e38.
24. Desai NA and V Shankar. (2003). Single-strand-specific nucleases. FEMS Microbiol Rev 26:457–491.
25. Dingwall C, GP Lomonossoff and RA Laskey. (1981). High sequence specificity of micrococcal nuclease. Nucleic Acids Res 9:2659–2673.
26. Horz W and W Altenburger. (1981). Sequence specific cleavage of DNA by micrococcal nuclease. Nucleic Acids Res 9:2643–2658.
27. Schnell FJ, SL Crumley, DV Mourich and PL Iversen. (2013). Development of novel bioanalytical methods to determine the effective concentrations of phosphorodiamidate morpholino oligomers in tissues and cells. Biores Open Access 2:61–66.
28. Arora V, DC Knapp, MT Reddy, DD Weller and PL Iversen. (2002). Bioavailability and efficacy of antisense morpholino oligomers targeted to c-myc and cytochrome P-450 3A2 following oral administration in rats. J Pharm Sci 91:1009–1018.
29. Hudziak RM, E Barofsky, DF Barofsky, DL Weller, SB Huang and DD Weller. (1996). Resistance of morpholino phosphorodiamidate oligomers to enzymatic degradation. Antisense Nucleic Acid Drug Dev 6:267–272.
30. Youngblood DS, SA Hatlevig, JN Hassinger, PL Iversen and HM Moulton. (2007). Stability of cell-penetrating peptide-morpholino oligomer conjugates in human serum and in cells. Bioconjug Chem 18:50–60.
31. Alter J, F Lou, A Rabinowitz, H Yin, J Rosenfeld, SD Wilton, TA Partridge and QL Lu. (2006). Systemic delivery of morpholino oligonucleotide restores dystrophin expression bodywide and improves dystrophic pathology. Nat Med 12:175–177.
32. Jarver P, T Coursindel, SE Andaloussi, C Godfrey, MJ Wood and MJ Gait. (2012). Peptide-mediated cell and in vivo delivery of antisense oligonucleotides and siRNA. Mol Ther Nucleic Acids 1:e27.
33. Laufer SD and T Restle. (2008). Peptide-mediated cellular delivery of oligonucleotide-based therapeutics in vitro: quantitative evaluation of overall efficacy employing easy to handle reporter systems. Curr Pharm Des 14:3637–3655.
34. Sazani P, F Gemignani, SH Kang, MA Maier, M Manoharan, M Persmark, D Bortner and R Kole. (2002). Systemically delivered antisense oligomers upregulate gene expression in mouse tissues. Nat Biotechnol 20:1228–1233.
35. Du L, R Kayali, C Bertoni, F Fike, H Hu, PL Iversen and RA Gatti. (2011). Arginine-rich cell-penetrating peptide dramatically enhances AMO-mediated ATM aberrant splicing correction and enables delivery to brain and cerebellum. Hum Mol Genet 20:3151–3160.
36. Pane M, R Scalise, A Berardinelli, G D'Angelo, V Ricotti, P Alfieri, I Moroni, L Hartley, MC Pera, *et al.* (2013). Early neurodevelopmental assessment in Duchenne muscular dystrophy. Neuromuscul Disord 23:451–455.
37. Perronnet C, C Chagneau, P Le Blanc, N Samson-Desvignes, D Mornet, S Laroche, S De La Porte and C Vaillend. (2012). Upregulation of brain utrophin does not rescue behavioral alterations in dystrophin-deficient mice. Hum Mol Genet 21:2263–2276.
38. Goodnough CL, Y Gao, X Li, MQ Qutaish, LH Goodnough, J Molter, D Wilson, CA Flask and X Yu. (2014). Lack of dystrophin results in abnormal cerebral diffusion and perfusion in vivo. Neuroimage 102 (Pt 2):809–816.

Address correspondence to:
Volker Straub, MD, PhD
The John Walton Muscular Dystrophy Research Centre
MRC Centre for Neuromuscular Diseases at Newcastle
Institute of Genetic Medicine
Newcastle University
Central Parkway
Newcastle upon Tyne NE1 3BZ
United Kingdom

E-mail: volker.straub@ncl.ac.uk

Received for publication December 12, 2014; accepted after revision June 2, 2015.